Impurity states in grain boundaries and adjacent crystalline regions. I. Temperature dependence of the population of states in the grain-boundary diffusion zone

V. N. Kaigorodov and S. M. Klotsman
Diffusion Phenomena Department, Institute of Metal Physics, Urals Divison of the Russian Academy of Sciences, 620219 Ekaterinburg, Russia

(Received 10 February 1992; revised manuscript received 29 April 1993)

We present the results of an investigation by emission nuclear γ-resonance spectroscopy of the population of states in the grain-boundary diffusion (GBD) zone. It is shown that atomic probes in polycrystals of some fcc and bcc metals only populate two discrete states in the GBD zone: one in the core of the grain boundary and one in the lattice sites adjacent to the grain boundary. For the typical fcc metals Pd, Pt, and Au, we investigated the dependence of the impurity-state populations on the temperature of the atomic-probe diffusion. It was shown that the "intrinsic" temperature dependence of state populations can be distorted owing to the formation of interstitial impurity segregation. In gold, where the volume solubility of such impurities is low, there is a temperature range of diffusion annealings, where the population-state regularities are determined by the "intrinsic" parameters of the atomic-probe diffusion. We made a suggestion concerning the atomic-probe diffusion mechanism in the interstitial impurity segregation zone, which causes the atomic-probe "pumping" parameters to change at low temperatures.

I. INTRODUCTION

One- and two-dimensional defects like dislocations and grain boundaries (GB) are being intensively investigated, since these defects play an essential role in the formation of important properties of real crystals. However, significant difficulties arise with investigations of such defects. They are caused by the fact that the density of states of electrons and ions that are bound to the core of the defect is very low. Therefore many experimental methods are unacceptable for studying these defects. The situation is still more complicated in metals. Conduction electrons effectively screen the defect perturbation potentials, substantially limiting the sizes of the "influence regions" surrounding the defect, which could be a source of information on the structure and properties of the defect core.

Methods based on the application of atomic probes (AP) acquire special importance under these circumstances. If it is possible to localize the AP (radioactive or stable isotopes, etc.) in the defect core, then the possibility arises of obtaining a measurable signal from the AP with practically zero background, in spite of the low average volume density of specific states of the defect core.

The use of AP's for investigation of grain-boundary diffusion (GBD) in metals allowed us to establish the following.[1-3]

(i) The temperature dependence of the parameter $W(\xi)$ for GBD in metals undergoes a break at temperature $(0.40-0.45)T_m$. Here, $W(\xi)=ds(\xi)D_{GB}(\xi)$, where $\xi=(RT_{diff})^{-1}$, $s(\xi)$ is the coefficient of AP segregation at the GB, d is the GB width, D_{GB} is the GBD coefficient (see Fig. 1), T_m is the matrix melting point, and T_{diff} is the diffusion temperature.

(ii) In the high-temperature range ($T>0.45T_m$), where the GBD regularities are determined by two fluxes (Fig. 1), fast diffusion along the grain boundary, and AP slow "pumping" into the adjacent crystallites, the following relation is satisfied:

$$Q_{GB}=(0.3-0.4)Q^{HT}_{pump}=(0.3-0.4)Q_{vol}\ , \qquad (1)$$

where Q_{GB}, Q^{HT}_{pump}, and Q_{vol} are the activation enthalpies of the GBD, of high-temperature (HT) pumping, and of volume diffusion, respectively. The equality $Q^{HT}_{pump}=Q_{vol}$ reflects the well-known fact that at high temperatures AP pumping is realized via volume diffusion. This allows us to use volume-diffusion parameters, measured on single crystals, for the calculation of diffusion parameters along the GB. Equation (1) indicates that in the GB core there is a diffusion mechanism that is different from the vacancy mechanism.

(iii) At the same high temperatures, the preexponential factor is

$$(D_{GB})^{HT}_0=10^{-3}\ \mathrm{cm^2/s}=(10^{-3}-10^{-2})(D_{vol})_0\ . \qquad (2)$$

Such a low value for $(D_{GB})^{HT}_0$ is naturally connected with the low activation entropy of diffusion along the GB,

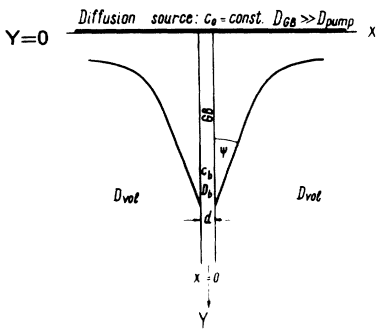

FIG. 1. Schematic presentation of the GB diffusion in a single slab, which is used as a model for the GB in a crystal.

which reflects in turn the softer spectrum of AP local oscillations in the GB core.

(iv) For impurities the GB diffusion activation enthalpy Q_{GB}^{HT} [as well as $(D_{GB})_0^{HT}$] increases with the growth of the excess charge of impurity Z_{21} (Fig. 2):

$$\partial Q_{GB}^{HT}/\partial Z_{21} > 0 , \tag{3}$$

unlike the analogous dependence for the volume-diffusion vacancy mechanism:

$$\partial Q_{vol}/\partial Z_{21} < 0 . \tag{4}$$

Relation (3) was theoretically established for interstitial diffusion of the positive excess charge in a metal.[4] The inequalities (3) and (4) prove the notion of the nonvacancy diffusion mechanism in the GB core.

(v) In the low-temperature range (LT) ($T < 0.4T_m$), the two-dimensional flux in the GB diffusion zone remains. This means that AP pumping from the GB core does not disappear even at such low temperatures (up to $T \cong 0.19T_m$),[5] at which the effective volume-diffusion length $X_D = 2(D_{vol}t)^{0.5} \cong 10^{-9}$ nm. Thus, in the low-temperature limit there comes into operation a new mechanism of AP pumping from the grain boundary into adjacent crystallites.

(vi) At these low temperatures,

$$Q_{pump}^{LT} \cong Q_{GB} \tag{5}$$

and

$$(D_{pump})_0^{LT} \cong (10^{-4}-10^{-3})(D_{GB})_0^{HT} .$$

These relations served as a base for the creation of the dislocation-pumping model.[1] But besides dislocations it is apparently necessary to take into account the impurity and vacancy segregations near the GB, which can also modify AP pumping from the GB at low temperatures. In this paper we present some results of investigation of the AP states, localized in the GBD zone, obtained by means of emission nuclear γ-resonance spectroscopy (NGRS).

II. METHODS AND MATERIALS

Here we list only the main characteristics of the method, giving a notion of the quality of the results. To establish the generality of results reported here we used single-atomic metals with fcc and bcc structure. Most of them are materials of 3N and 4N purity. The tungsten polycrystals were produced by cool rolling and subsequent recrystallization of high-purity ($R_{4.2}/R_{300} \cong 10^5$, where R_T is the electroresistance at temperature T) single crystals.

Before the diffusion source was made, the purity of the prepared samples was checked by secondary-ion mass spectrometry on the IMS-3f ion microanalyzer, CAMECA, France. Purification with etching was carried out until substitutional-impurity content in the surface layers was as low as the volume content.

For qualitative characterization of GB types in polycrystals, a texture analysis of tungsten and platinum samples was conducted. It was established that in cold-rolled and recrystallized tungsten there was formed one component, namely, the "sharp" texture of the type with the (222) plane parallel to the extrinsic surface. This means that in polycrystalline tungsten, as made by us, the small-angle GB's predominate.[6] In rolled and recrystallized platinum foils, there were practically no preferential grain orientations. This indicates that large-angle GB's are predominant in polycrystals of fcc metals.

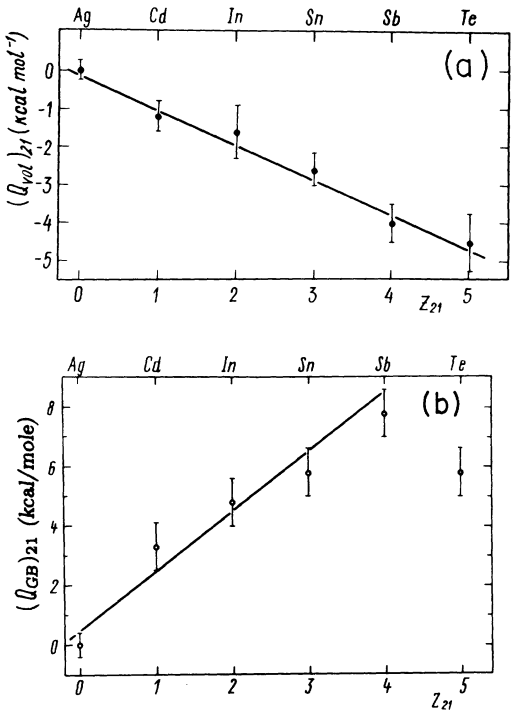

FIG. 2. Curves of the differences $Q_2 - Q_1 = Q_{21}$ of the diffusion activation enthalpies vs AP excess charge Z_{21} for (a) volume and (b) GB diffusion for 5sp impurities in silver (Refs. 1,2).

To create the diffusion source, we used a preparation of ^{57}Co with specific activity of 10^4 Ci/g. We removed some cation impurities with ion-exchange resins. ^{57}Co was deposited onto the surfaces of samples electrolytically. Diffusion annealings were carried out in quartz tubes, which were pumped continuously by turbomolecular pumps, in a vacuum of about 10^{-5} Pa. After annealing, the residual undiffused ^{57}Co was eliminated by etching. After that the surface layer of the sample was removed by a suitable method for each matrix etchant. The thickness of the removed layer was about 1×10^{-4} cm, which greatly exceeded the volume-diffusion depth $X_D = 2(D_{vol}t)^{0.5}$.

Samples prepared in this way were placed into the cryostat of the constant-rate NGR spectrometer. NGRS measurements were accomplished over the temperature range of 5.5–300 K. Potassium ferrocyanide enriched with ^{57}Fe was used as an absorbent, which for all measurements was at room temperature. While analyzing NGR spectra, we assumed that all NGRS components have Lorentz shape.

III. GENERAL DESCRIPTION OF NGR SPECTRA FROM POLYCRYSTALS

If, after diffusion annealing of the polycrystal, the AP quantity in the GB core is comparable with the AP quantity in the pumping regions at both sides of the GB, we expect the following: the occurrence of only one component in the NGR spectrum, which is caused by AP states of type 1 in lattice sites in the pumping zone; and the occurrence of one or a few components in the NGR spectrum, which are caused by AP states of type 2, localized in the GB core.

It is obvious that, with the change of diffusion temperature (T_{diff}), the population of these states must change because of the differences in diffusion activation enthalpies in the corresponding regions. Accordingly, a change of the intensities A_i of these two NGRS components must be observed. So, the NGRS component caused by AP type-1 states in the pumping zone has to be the only one in the NGR spectrum, until the number of occupied states in the pumping zone (at high T_{diff}) remains much larger than the number of type-2 states occupied in the GB core. At high T_{diff} ($T_{\text{diff}} > 0.5T_{\text{melt}}$) one can obtain information only on the structure and properties of type-1 states localized in the pumping zone.

At intermediate T_{diff} ($T_{\text{diff}} \cong 0.35T_m$), at which the AP quantities in the pumping zone and the GB core become comparable, new components appear in the NGR spectrum. Their occurrence is accompanied by a drop of the A_1 areas (area of NGRS component 1 results from type-1 states). The relative decrease of population of type-1 states in the pumping zone takes place because of the higher pumping activation enthalpy in comparison with the diffusion activation enthalpy in the GB core [see Eq. (1)].

At lower T_{diff} ($T_{\text{diff}} < 0.3T_m$), the character of the NGR spectra from polycrystals depends on preservation of the pumping mechanism by volume diffusion. If this pumping mechanism remains also at low T_{diff} (we name this situation "intrinsic"), then we must expect the disappearance of line 1 and the saturation of the line-2 area. However, if the mechanism of AP pumping from the GB changes at low T_{diff}, as has been established in diffusion experiments (see the Introduction), then the temperature dependence of the state populations in the GBD zone must be changed.

For a quantitative description of the populations of states in the GBD zone, let us use the simplest but correct GB diffusion description in the Goldstein-Fisher (GF) approximation.[7,8] The number of AP's in the GB core is given by (Fig. 1):

$$F_2 = q_2 N = P \int_{-d}^{0} \partial x \int_0^{\infty} C_0 \exp(-\alpha_{\text{GF}} y)\partial y = PC_0 d\alpha_{\text{GF}}^{-1} . \tag{6}$$

Here $\alpha_{\text{GF}} = -\partial \ln C/\partial y = [(sdD_{\text{GB}})^{-1}(D_{\text{pump}}/\pi t)^{0.5}]^{0.5}$, N is the number of AP's in the sample, q_2 is the population of type-2 states, P is the perimeter of GB's in the diffusion source plane. The AP quantity in the pumping zone is

$$\begin{aligned} F_1 &= q_1 N \\ &= 2PC_0 \int_0^{\infty} \operatorname{erfc}(x/X_{\text{pump}})\partial x \int_0^{\infty} \exp(-\alpha_{\text{GF}} y)\partial y \\ &= 2PC_0 X_{\text{pump}} \alpha_{\text{GF}}^{-1} . \end{aligned} \tag{7}$$

Here, the pumping depth $X_{\text{pump}} = 2(D_{\text{pump}}t)^{0.5}$. Hence, the relative AP quantity equal to the AP state population in the GB core is

$$\sigma_2 = F_2/(F_1+F_2) = q_2/(q_1+q_2) = d/(d+2X_{\text{pump}}) , \tag{8}$$

and in the pumping zone,

$$\begin{aligned} \sigma_1 &= F_1/(F_1+F_2) = q_1/(q_1+q_2) \\ &= 2X_{\text{pump}}/(d+2X_{\text{pump}}) . \end{aligned} \tag{9}$$

It is easy to see that the populations of these two states are equal to the relative volumes of the regions where these states are localized. This simplifies considerably a possible generalization of this phenomenological description. The important result of this consideration is the independence of the relative populations σ_1 and σ_2 on diffusion parameters in the GB core: the magnitudes σ_1 depend on the parameters of pumping only.

For experimental determination of the relative population of the type-i state, let us use the definition of the component area A_i in the NGR spectrum:[9]

$$A_i = \phi q_i f_i . \tag{10}$$

Here ϕ is the NGR spectrometer parameter, q_i is the type-i state population, and f_i is the NGR probability in state i. It is easy to show that the parameter of interest to us, the relative population σ_i of state i, is

$$\sigma_i \equiv q_i = A_i/(A_i + A_j f_i/f_j) . \tag{11}$$

IV. THE TEMPERATURE DEPENDENCE OF THE STATE POPULATION IN THE GBD ZONE

The analysis of the "intrinsic" situation, which led to expressions (8) and (9), may be generalized for the case of the "extrinsic" situation, in which a change of diffusion parameters in the GBD zone occurs because of impurity segregation or dislocation pumping. We see from (8) and (9) that the relative population σ_i does not depend on D_{GB}. Then one can take into consideration the segregation influence only on the pumping characteristics. It is well known that in highly diluted solid solutions, to which metals of 3N and 4N purity belong, the concentration of residual impurities in the segregation zone may be approximated by

$$C_{\text{segr}} = C_{\text{sol}} \exp(Q_s \xi) . \tag{12}$$

Here, C_{segr} is the concentration of segregated impurities near the GB, C_{sol} is the concentration of this impurity in solid solution, and Q_s is the segregation activation enthalpy.

To keep in the framework of the description created by expressions (8) and (9), let us introduce the volume (thickness) of the segregation layer X_s, which is assumed to be proportional to the average concentration in this layer:

TABLE I. Phenomenological description of state-population relationships in the GBD zone.

Characteristics of $\sigma(\xi)$ dependencies	Intrinsic case	Extrinsic case
Appearance of line 2 $\sigma_2 \leq 0.1\sigma_1$	$d \leq 0.1X_D$	$d \leq 0.1(X_D+X_s)$
	$\xi_{intr}(AT) < \xi_{extr}(AT)$	
Activation enthalpy at appearance temperature (AT) $Q(\sigma_2)\|_{0.1\sigma_1}$	$Q(\sigma_2) = -\partial \ln\sigma_2/\partial\xi$	
	$-0.9Q_D/2$	$Q(\sigma_2) - \|A\|$
	$Q(\sigma_2)_{intr} > Q(\sigma_2)_{extr} - \|A\|$	
$\sigma(\xi)$ without intersection point (IP)	$\sigma_1 > \sigma_2$ at all ξ	
	Impossible	$d < X_D + X_s$
$\sigma(\xi)$ with IP, $\sigma_1 = \sigma_2$	$d = X_D\|_{IP}$	$d = (X_D+X_x)\|_{IP}$
Position of IP	$\xi_{int} = Q_D^{-1}\ln(tD_0/d)$	$\xi_{ext} = \xi_{int} + \ln(1+X_s/X_D)$
Activation enthalpy at IP	$-Q_D/4$	$Q^{IP}_{intr} - \|B\|$
	$Q^{IP}_{intr} > Q^{IP}_{extr}$	
$\sigma(\xi)$ with IP and with extremum at $\xi_{IP} < \xi$	Impossible	$X_D Q_D/2 = X_s Q_s$
$\sigma(\xi)$ with IP, but without extrema: triple point	$\sigma_1 \cong \sigma_2$ at all $\xi_{IP} < \xi$	
	Impossible	$d \cong X_D + X_s$ or $X_s = \text{const} \cong d$

$$X_s = \text{const} \times C_{segr} = (X_s)_0 \exp(Q_s\xi) \ . \tag{13}$$

Finally, we assume that the pumping region volume (thickness) X_{pump} in the extrinsic case is equal to the sum of the volumes (thicknesses) of the segregation layer, X_s, and the layer of pumping by means of the volume-diffusion mechanism, X_D.

Table I represents the main relationships of σ_i with respect to change of ξ. Let us mark some of the most important features of the curves $\sigma(\xi)$. First of all, three types of curves are possible in the presence of the segregation layer, unlike the intrinsic case presented schematically in Fig. 3. Curves of type I have no intersection point (IP) of curves σ_1 and σ_2. Curves of type II have an intersection point, but without extrema in the $\sigma_i(\xi)$ curves. Curves of type III have an intersection point and extrema in both curves.

In Fig. 4 all three types of curves are shown schematically. The curve of type I appears when the value X_s is larger than values X_D and d for any T_{diff}. The curves II and III with intersection points are basically rudiments of the intrinsic curve. However, the position of the intersection point (IP), ξ(IP), appears to be displaced for them:

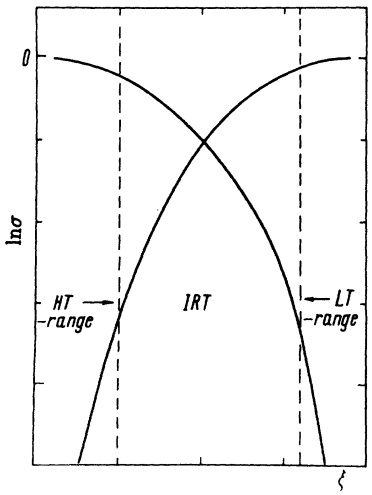

FIG. 3. Schematic dependencies $\ln\sigma(\xi)$ for the intrinsic case.

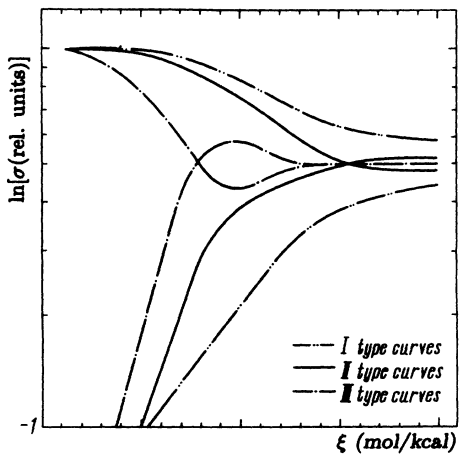

FIG. 4. Schematic dependencies $\ln\sigma(\xi)$ for different extrinsic cases: types-I, -II, and -III curves.

$$\xi_{\text{intr}}(\text{IP}) < \xi_{\text{extr}}(\text{IP}) . \quad (14)$$

Moreover, even the appearance temperature (AT) of line 2, ξ(AT), appears to be displaced, because the pumping parameters are changed due to the segregation

$$\xi_{\text{intr}}(\text{AT}) < \xi_{\text{extr}}(\text{AT}) . \quad (15)$$

Correspondingly, the pumping activation enthalpy $Q(\sigma_2)$, calculated from the $\ln\sigma_2(\xi)$ dependence and determined on the $0.1\sigma_1$ level (a line-2 AT) appears to be changed too. Now in the extrinsic case we have

$$Q(\sigma_2, 0.1\sigma_1)_{\text{extr}} < Q(\sigma_2, 0.1\sigma_1)_{\text{intr}} . \quad (16)$$

Let us turn now to the experimental NGR spectra, measured after various T_{diff} for representative samples of bcc and fcc metals (Figs. 5–10). In all spectra one observes the relationship discussed: with decrease of T_{diff} (with growth of ξ) there is a decrease in the intensity of the line, which was the only one at high T_{diff}. This, naturally, is the line 1, caused by AP states of type 1 in the pumping region, in sites of the regular lattice adjacent to the GB. At some temperature there appears one new line, which grows in area as T_{diff} is decreased further. However, after reaching a certain value of T_{diff}, where the areas of the two lines are equal, the change of magnitude of σ_i stops.

The most important result here is that there is only one line 2, caused by only one kind of type-2 state in the GB core, which the AP occupies during diffusion into a polycrystal. The properties of lines 2 and the type-2 states giving rise to them will be discussed in detail in a separate publication.[10] As we see, a diffusion filter caused the population of only one of the collection of type-2 states in the GB core. This is a result of the choice of the minimum potential-barrier height by the diffusing AP's. After diffusion annealing, the AP's are fixed in equilibrium positions, which form the lowest potential barriers.

In Figs. 11–15 we present the typical experimental dependencies $\sigma(\xi)$. Here one observes all the types of

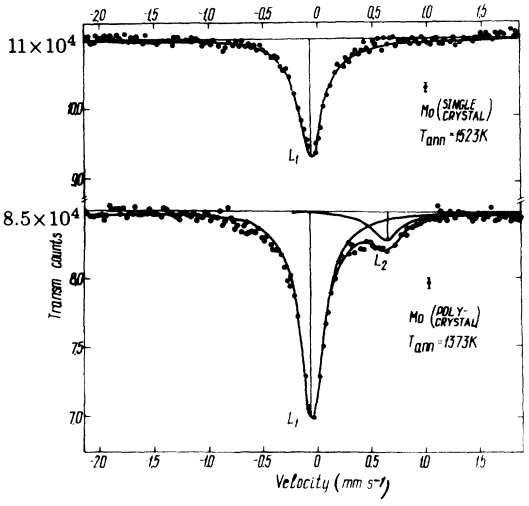

FIG. 5. Emission NGRS for Mo single crystal and polycrystal after annealing at different T_{diff}.

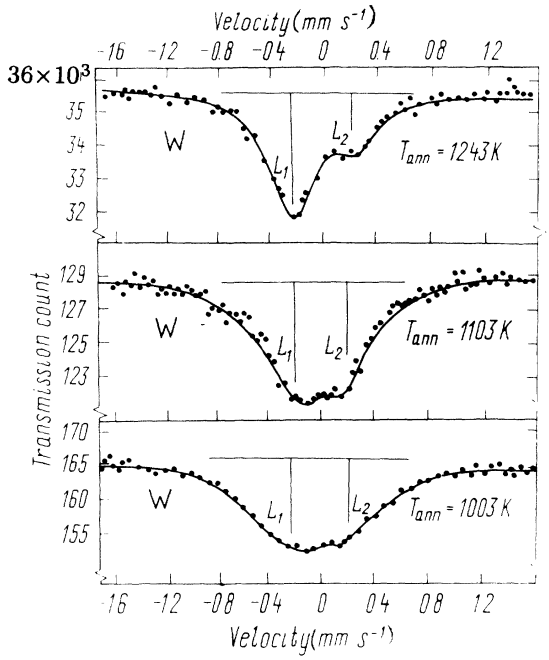

FIG. 6. Emission NGRS for W polycrystals after annealing at different T_{diff}.

curves discussed above. Hence one can conclude that a simple model of AP state population in a polycrystal, which consistently takes into account the possibility of formation of an impurity segregation layer near the GB and the dependence of concentration and volume (thickness) of the segregation layer on T_{diff}, describes exhaus-

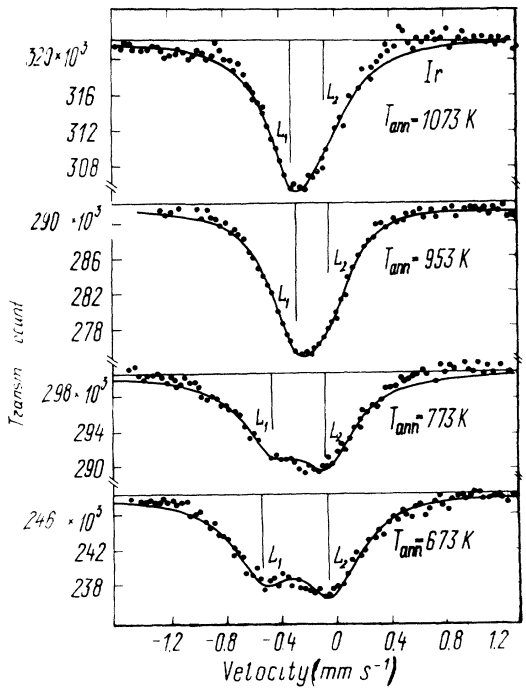

FIG. 7. Emission NGRS for Ir polycrystals after annealing at different T_{diff}.

tively the experimental situation.

Let us show that the main conclusions of the model used are confirmed by experiment. For this let us estimate the lower boundary of the intrinsic, high-temperature region (the highest value of $\xi - \xi_{\max}^{\text{intr}}$) up to which we can determine the intrinsic properties of states in the GBD zone. The obvious criterion of the intrinsic situation is

$$X_s, d \ll X_D \quad \text{or} \quad d \leq 0.1 X_D \ . \tag{17}$$

For analyzing the intrinsic situation, we use as pumping parameters the parameters of volume diffusion of Co in Au and Pt.[11] For Pd, in which the volume diffusion of Co was not measured, we use volume self-diffusion parameters.[11] The basis of such a substitution is the following. It is known that Co has unlimited solubility in Ni-group metals, which is evidenced by the similarity of physical properties of these metals. Besides, it has been shown experimentally that activation enthalpies of self- and heterodiffusion of Co in Ni coincide.[12]

Table II presents the theoretical estimations of $\xi_{\max}^{\text{intr}}$. It is seen that they differ essentially for the three metals. In gold, both ξ(AT) and even ξ(IP) appear in the region

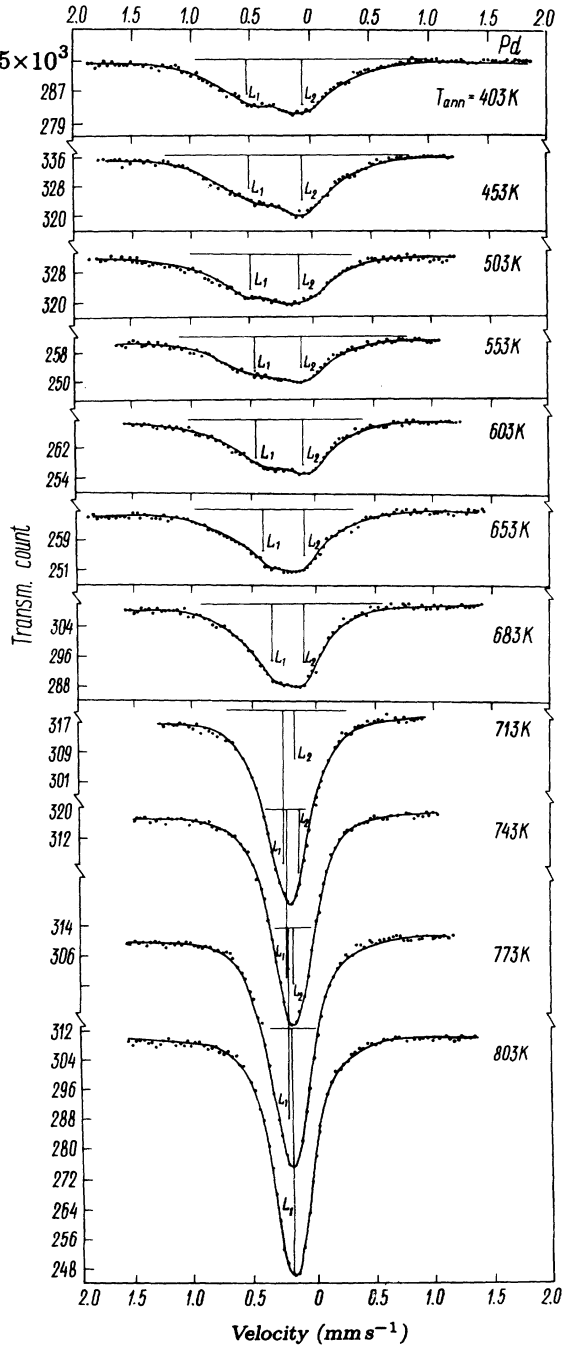

FIG. 8. Emission NGRS for Pd polycrystal after annealing at different T_{diff}.

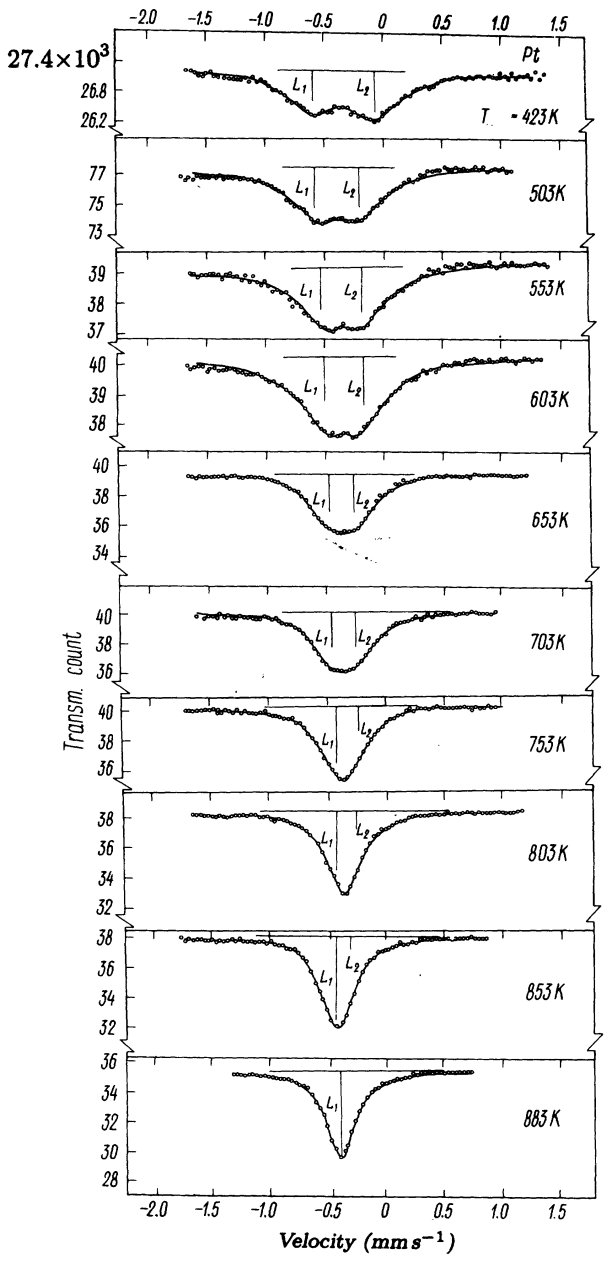

FIG. 9. Emission NGRS for Pt polycrystal after annealing at different T_{diff}.

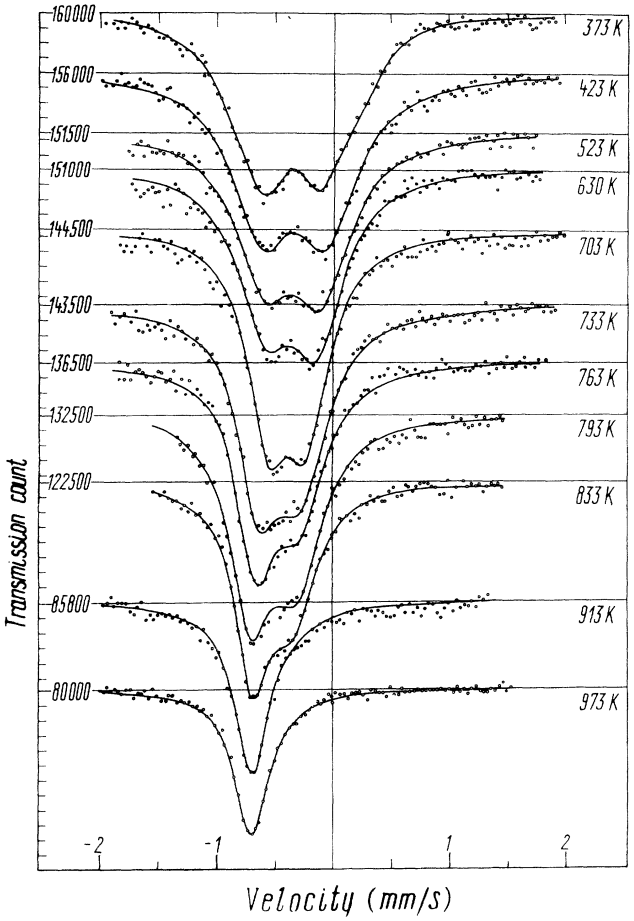

FIG. 10. Emission NGRS for Au polycrystal after annealing at different T_{diff}.

where it is possible to determine intrinsic parameters of GBD from the dependencies $\sigma_2(\xi)$. However, for Pt and Pd even the experimental values $\xi(\text{AT})$ are essentially higher than estimated values of $\xi_{\max}^{\text{intr}}$.

In Table III we present the pumping activation enthalpies, defined by the initial parts of the dependencies

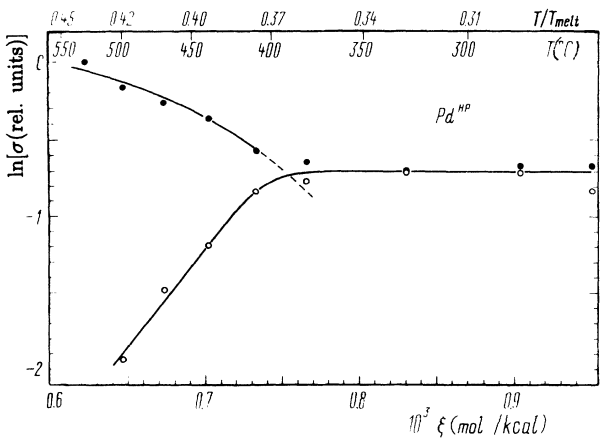

FIG. 11. Experimental dependencies $\ln\sigma(\xi)$ for polycrystalline Pd.

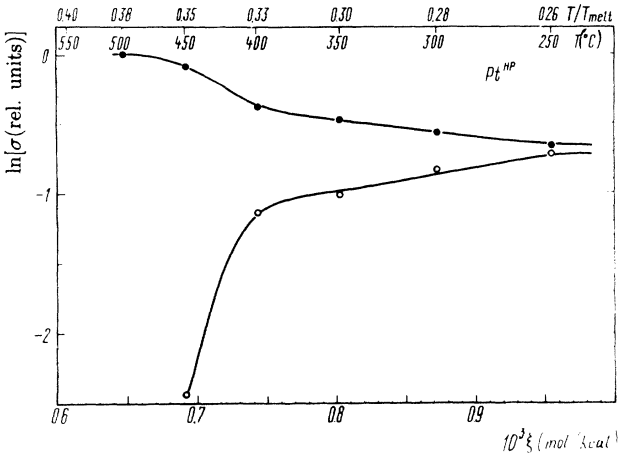

FIG. 12. Experimental dependencies $\ln\sigma(\xi)$ for polycrystalline Pt (type I).

$\sigma_2(\xi)$. It is seen, in full accordance with conclusions drawn earlier (Table I), that the values $Q_{\text{pump}}^{\text{HT}}$ in Pd and Pt are about 1.5 times smaller than the values of Q_{vol}. But in Au these values coincide surprisingly exactly, especially if one takes into account the small number of points used in determining the dependence $\sigma_2(\xi)$. Hence, one can conclude that in the pumping zone of gold no segregation of such impurities arises, which are responsible for the change of the pumping mechanism at low temperatures.

V. POSSIBLE PUMPING MECHANISM AT LOW DIFFUSION TEMPERATURES

Before going to the discussion of possible pumping mechanisms at low T_{diff}, let us sum up the main features of the dependencies $\sigma(\xi)$, which may be used to obtain information we are interested in. We discovered three types of dependencies $\sigma(\xi)$. All three types can be described on the basis of a few results: the relative state population σ_i in the GBD zone is equal to the relative

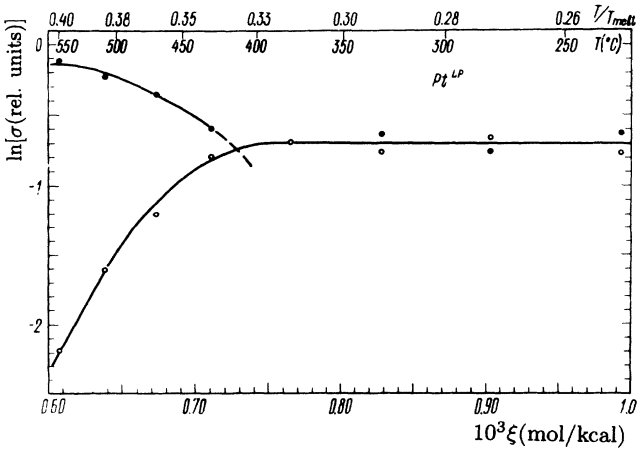

FIG. 13. Experimental dependencies $\ln\sigma(\xi)$ for polycrystalline Pt (type II).

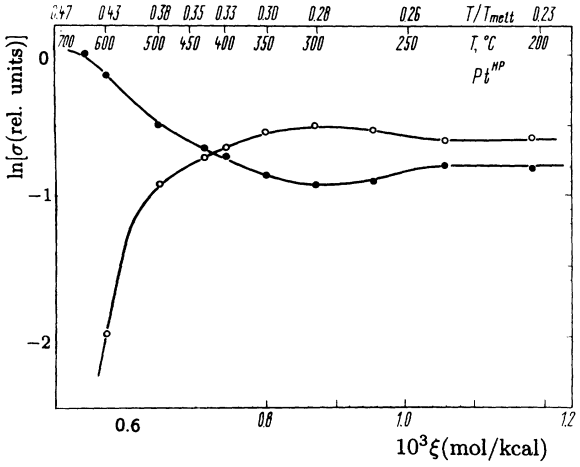

FIG. 14. Experimental dependencies $\ln\sigma(\xi)$ for polycrystalline Pt (type III).

volumes of the regions in which these states are localized; and the volume of the type-1 localization region is the sum of two independent items. These are the volume X_s of the segregation (of vacancies, impurities, and their complexes) region, which increases exponentially in some temperature interval with the growth of ξ, and the volume X_D of region where the mechanism of volume diffusion is realized, which decreases exponentially with the growth of ξ at all temperatures.

Although the extrinsic features of the dependencies $\sigma(\xi)$ show that all of them are complicated by extrinsic effects to some degree, the pumping parameters in the high-temperature limit, defined from the dependencies $\sigma(\xi)$ for gold, coincide well with the parameters of volume diffusion of Co in Au. On the other hand, the pumping parameters for Pd and Pt, similarly defined, are much smaller than the volume diffusion parameters in these metals. This appears to be natural, taking into account all features of the extrinsic shape of the $\sigma(\xi)$ curves. Therefore one can infer that the shapes of the $\sigma(\xi)$ curves, measured on gold, which can be considered

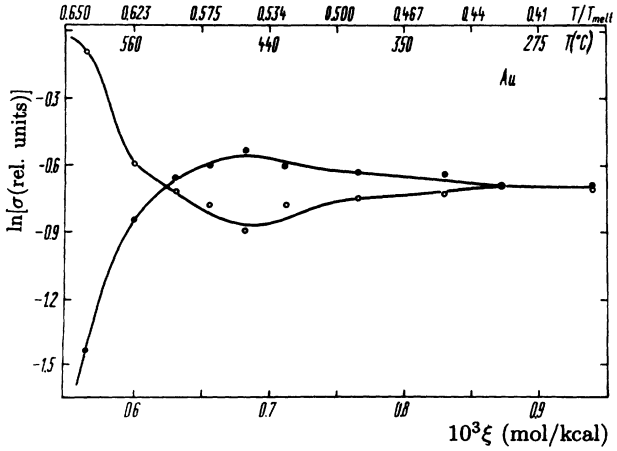

FIG. 15. Experimental dependencies $\ln\sigma(\xi)$ for polycrystalline Au.

TABLE II. Estimations and experimental parameters of dependencies $\sigma(\xi)$ for some fcc metals All diffusion parameters are from Ref. 11, $\xi_m=(RT_m)^{-1}$.

Matrix	Au		Pt		Pd
Type of $\sigma(\xi)$	III	I	II	III	II
Q_{SD} (kcal/mol)	41.60		61.54		63.60
Q(Co) (kcal/mol)	44.24		74.22		Fe:62.10
D_0(Co) (cm^2/s)	0.25		19.6		Fe:0.18
$10^4\xi^{intr}_{max}$ (kcal/mol)$^{-1}$	8.7		5.8		6.0
$10^4\xi$(AT) (kcal/mol)$^{-1}$	6.0	7.0	6.1	5.6	6.5
ξ_m/ξ(AT)	0.62	0.35	0.40	0.44	0.42
$10^4\xi$(IP) (kcal/mol)$^{-1}$	6.35		7.30	7.30	7.55
ξ_m/ξ(IP)	0.60		0.33	0.33	0.37

as a display of the qualitative features of the extrinsic situation, have some other origin, not connected with impurity segregation.

Thus, one can describe all features of the $\sigma(\xi)$ dependencies in Pd and Pt on the basis of the extrinsic effect—the occurrence of segregation and variation of the segregation-layer thickness with diffusion temperature. We must conclude that for gold there are no signs of the occurrence of the same segregation as in Pd and Pt. It is necessary to find a different mechanism of low-temperature pumping to account for the extrinsic shape of the curves $\sigma(\xi)$ in Au.

The mechanism of dislocation pumping was examined in Ref. 1. At low temperatures, pumping by volume diffusion becomes low. This makes the pumping from GB's by lattice dislocations, which cross or decorate the GB's, competitive with volume diffusion. As is shown in Ref. 1, this pumping mechanism explains completely the breaks in the dependencies $W(\xi)$. The main point is that for such a pumping mechanism Eq. (1) is satisfied which is necessary and sufficient to fulfill the condition $\sigma_1\cong\sigma_2$ at low temperature (Table I).

The only difficulty in the way of using the dislocation pumping is the absence of any effects in NGR spectroscopy, which would display the population of new states localized in the dislocation core. However, it may be shown that the relative volume in which these new AP states are localized is negligibly small in comparison with

TABLE III. Diffusion pumping activation enthalpies of ^{57}Co in some fcc metals determined from $\sigma_2(\xi)$ dependencies. $Q(\sigma_2)\equiv Q(\sigma_2)|_{0.1\sigma_1}=-\partial\ln\sigma_2|_{0.1\sigma_1}/\partial\xi$, $Q^{intr}_{pump}=Q_D=2Q(\sigma_2)/0.9$ as defined in Table I. Estimation of the pumping activation enthalpies for these matrices was made with these expressions. The $Q(\sigma_2)$ values were determined from graphical slopes at points $\sigma_2\cong0.1\sigma_1$ of curves $\ln\sigma(\xi)$, which were drawn by eye. Therefore the errors of these values are unknown.

	Au	Pt		Pd
		low purity	high purity	
T_{diff}/T_{melt}	0.38–0.44	0.38–0.40		0.42
$Q(\sigma_2)$ (kcal/mol)	20	19	20	19
Q_{pump} (kcal/mol)	44	42	44	42
Q(Co) (kcal/mol)	44.2	74.22		63.6

the volume of the GB core. The average lattice-dislocation density in well-annealed polycrystal is $n \cong 10^5 - 10^7$ cm^{-2}. Then the absolute volume of dislocations, by which pumping from the GB is realized, is

$$V_{\text{disl}} \cong n \pi r^2 S_{\text{GB}} X_{\text{disl}} \ . \tag{18}$$

Here $r = 5 \times 10^{-8}$ cm is the radius of the dislocation core, $S_{\text{GB}} = PY_{\text{GB}}$ is the GB surface from which the AP diffused in the pumping dislocation, Y_{GB} and X_{disl} are the depths of AP diffusion along the GB and dislocation cores, respectively. In the same approximation, the absolute volume of the GB core, populated by the AP, is $V_{\text{GB}} \cong dPY_{\text{GB}}$. Here $P \cong 2/L^2$ is the perimeter of the GB's in the diffusion source plane and L is the grain size. Then, as $X_{\text{disl}} \cong Y_{\text{GB}}$, the following expression may be derived:

$$V_{\text{disl}}/V_{\text{GB}} \cong n \pi r^2 X_{\text{disl}}/d \cong 10^{-6} - 10^{-4} \ . \tag{19}$$

It is obvious that such a low state density cannot be registered by NGRS. Thus, dislocation pumping may be displayed in the "impurity-free" situation only as a shape change of the $\sigma(\xi)$ dependencies, but the detection of a new spectral component connected with dislocation core states is impossible.

To summarize this section, we have pointed out the most likely mechanism which can provide the necessary pumping parameters in the impurity segregation zone. To explain the represented results it is necessary that in the segregation layer a high vacancy concentration be present, which must be independent of diffusion temperature. The pumping activation enthalpy would be roughly equal to the vacancy-migration activation enthalpy, which in fcc metals is about one-half of the self-diffusion activation enthalpy.

A polyvalent substitutional impurity cannot be considered as a suitable partner for the creation of vacancy-impurity complexes (VIC's) in the segregation zone. The bond energies of vacancies with polyvalent substitutional impurities in metals are relatively small: about 2–3 kcal/mole. This means that VIC's formed on the base of polyvalent substitutional impurities are not stable at temperatures used by us.

Moreover, it is known that NGR spectra are only weakly sensitive to alloying of metals with substitutional impurities. So the doping of Pt up to 20 at. % with Fe does not change the position of the single paramagnetic line on the velocity scale.[13] It is obvious that the vacancy concentration in the segregation layer is many orders lower than this value. Thus, one can be sure that, in case of segregation of the vacancies or of their complexes with substitutional impurities, we must observe the unchanging position of line 1 in the NGR spectrum. However, in most metals, including Pd and Pt, both lines of the NGR spectrum are shifted on the velocity scale (see Figs. 5–10). Therefore, the segregation layer in those metals contains not only vacancies and substitutional impurities, but also such impurities which change the isomer shift (IS) of type-1 states. Such impurities, small concentrations of which induce the IS change noticed, are the interstitial impurities.

Thus, for example, in solid solutions of hydrogen in Pd(^{57}Fe) (Ref. 14) and Ta(^{181}Ta) (Ref. 15) systems, the IS decreases linearly with the growth of the hydrogen concentration C(H). Such behavior is caused by a simple circumstance. In solid interstitial solutions the lattice parameter and volume at the lattice site increase. If the AP's populates such a site, then its atomic volume increases. This leads to a decrease of self-s-electron density at the AP nucleus. The latter circumstance is the reason for the IS decrease in emission NGRS with ^{181}Ta or with ^{57}Co.

For an explanation of the presented results it is necessary to take into account two types of point defects segregated near the GB. These are the vacancies in high concentration (necessary for ^{57}Co pumping from the GB at low T_{diff}) and the interstitial impurities in concentration nearly equal to the vacancy concentration (for formation of stable VIC's). It is just such a situation that evidently occurs in metals of the Ni group. It is shown in Refs. 16 and 17 that the solubility of interstitial impurities like hydrogen, carbon, oxygen, etc., in metals of this group reaches several percent. It has been established experimentally that at low temperatures, when these impurities become oversaturating, the vacancy–interstitial-impurity complexes form. Since it is necessary to find enough vacancies to bond all the interstitial impurities, then near the GB's, which are vacancy sources, the interstitial impurities find their partners to form VIC's. As is shown in Refs. 16 and 17, carbon segregates near GB's and dislocations and decorates all possible vacancy sources. Such VIC's have a high bond energy of about 12–18 kcal/mole. It is obvious that near the vacancy sources the VIC concentration will be defined only by the concentration of the interstitial impurities which reached these regions, and by the bond energy of the complexes. This provides almost a constant VIC concentration in the temperature range investigated by us.

The existence of the segregation layer enriched with VIC's creates a unique set of conditions for AP pumping. Here the situation becomes the same as in ionic crystals in the impurity region of self-diffusion. The presence of

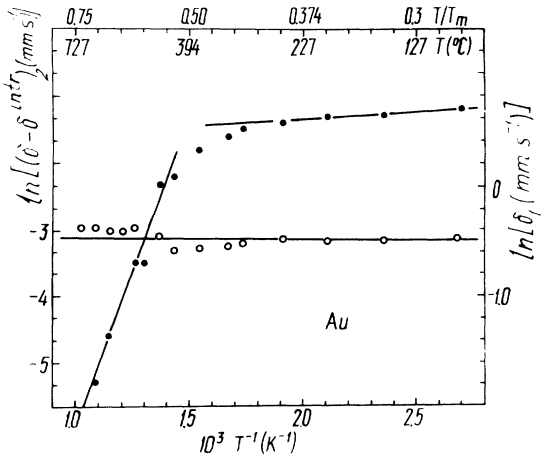

FIG. 16. Curves of $\ln\Delta\delta(T^{-1})$ for polycrystalline Au. (Open circles: δ_1 points right scale, closed circles: δ_2 points left scale.)

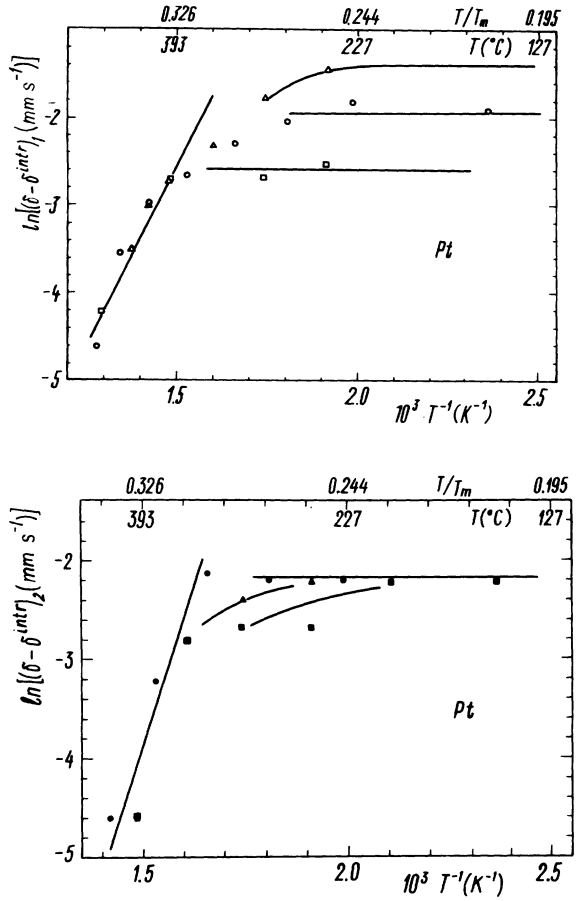

FIG. 17. Curves of $\ln\Delta\delta(T^{-1})$ for polycrystalline Pt.

polyvalent impurities in ionic crystals is the reason for VIC formation with vacancies of opposite charge. The concentration of vacancies bonded with polyvalent impurities is many orders higher than their equilibrium concentration at such low temperatures. Self-diffusion at this low T_{diff} is realized by VIC's and the activation enthalpy decreases by a factor of 2 and becomes equal to the vacancy-migration activation enthalpy.[18]

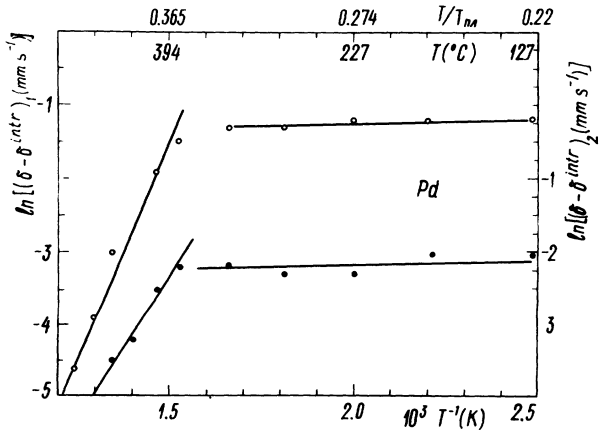

FIG. 18. Curves of $\ln\Delta\delta(T^{-1})$ for polycrystalline Pd. (Open circles: δ_1 points, closed circles: δ_2 points.)

TABLE IV. Segregation activation enthalpies (kcal/mol) of vacancy-impurity complexes for two types of AP states in the GBD zone of some fcc metals.

Matrix	Pd	Pt	Au
Q_{1s}	18	25	. . .
Q_{2s}	11	18	19

All the same effects occur in segregation layers containing VIC's in metals. The activation enthalpy of AP diffusion in the pumping zone will halve and reaches the level of the diffusion activation enthalpy in the GB core, as was established by us earlier [see Eq. (1)].

We will use the experimentally linear relation[15] between IS values for the substitutional AP ^{181}Ta and concentration of the classical interstitial impurity hydrogen in the solid solution Ta(H) for calculating the parameters of temperature dependence of the interstitial-impurity segregation. We use the assumption that also in our case:

$$C_{\text{segr}} \sim (\delta - \delta_{\text{intr}}) , \tag{20}$$

where δ_{intr} is the IS for intrinsic type-1 states which can be detected at high T_{diff} in polycrystals. Figures 16–18 show the curves of $\ln(\delta - \delta_{\text{intr}})$ vs T^{-1} for gold, platinum, and palladium. As can be seen, for gold the δ_1 is practically independent of T_{diff}. This means that in the pumping zone near the GB in gold the segregation of interstitial impurities is absent, in full accordance with our earlier conclusions. But in the GB core, in regions of localization of type-2 states, the IS varies with T_{diff}. The linear part of the curve of $\ln(\delta - \delta_{\text{intr}})$ vs T^{-1} can be used for determination of the segregation activation enthalpies for each of the investigated states Q_{si}:

$$Q_{si} = \partial \ln(\delta_i - \delta_{\text{intr}})/\partial\xi . \tag{21}$$

We assume that the linear relation (20) is correct not only for substitutional AP's but also for interstitial AP's, that is, for type-2 states. This is because in both situations the leading interactions are the elastic interactions of interstitial impurities with AP's, which are located either in lattice sites (states of type 1) or in interstitial positions in the GB core (states of type 2). Table IV shows the values of segregation activation enthalpies. As can be seen, these values are very close to the bonding energies of the interstitial impurities with vacancies measured in Refs. 16 and 17. This indicates that the segregation of VIC's disappears when interstitial impurities leave VIC's. Thus, consideration of the features of point-defect interactions leading to the formation of VIC's near vacancy sources (GB's) enables us to explain the temperature dependence of state populations in the GB diffusion zone and to understand the origin of breaks in the temperature dependencies $P(\xi)$ of the GB diffusion parameter $W(\xi)$.

ACKNOWLEDGMENT

The authors thank Professor S. V. Vonsovsky for help.

[1]V. N. Kaigorodov *et al.*, Fiz. Met. Metalloved. **25**, 910 (1968).
[2]V. N. Kaigorodov *et al.*, Fiz. Met. Metalloved. **27**, 1048 (1969).
[3]V. N. Kaigorodov *et al.*, Fiz. Met. Metalloved. **24**, 661 (1967).
[4]S. J. Fuyita, J. Phys. Chem. Solutions **49**, 41 (1988).
[5]N. K. Arkhipova *et al.*, J. Appl. Phys. **72**, 454 (1992).
[6]A. N. Orlov *et al.*, *Grain Boundaries in Metals* (Metallurgie, Moskow, 1980).
[7]T. Yu. Goldstein, Ph.D. thesis, Sverdlovsk University, USSR, 1951.
[8]J. C. Fisher, J. Appl. Phys. **22**, 74 (1951).
[9]G. N. Belotherskii, *Mössbauer Spectroscopy as a Method of Surfaces Investigations* (Energoisdat, Moskow, 1990), p. 44.
[10]V. N. Kaigorodov and S. M. Klotsman, this issue, Phys. Rev. B **49**, 9395 (1994).
[11]*Diffusion in Solid Metals and Alloys*, edited by H. Mehrer, Landolt-Bornstein, Group 3, Vol. 26 (Springer-Verlag, Berlin, 1990).
[12]V. N. Kaigorodov *et al.*, Fiz. Met. Metalloved. **46**, 1239 (1978).
[13]G. Bemski *et al.*, Phys. Lett. **18**, 213 (1965).
[14]J. S. Carlow and R. E. Meads, J. Phys. F **2**, 982 (1972).
[15]A. Heidemann *et al.*, Phys. Rev. Lett. **36**, 213 (1976).
[16]K. H. Westmacott *et al.*, Metall. Trans. A **17**, 807 (1986).
[17]C. Koster *et al.*, Scr. Metall. **20**, 1775 (1986).
[18]N. L. Peterson and S. J. Rothman, Phys. Rev. **177**, 1329 (1969).